RECENT RESULTS IN STRANGENESS PHOTO AND ELECTROPRODUCTION

(A BRIEF SURVEY)

Daniel S. Carman
Ohio University

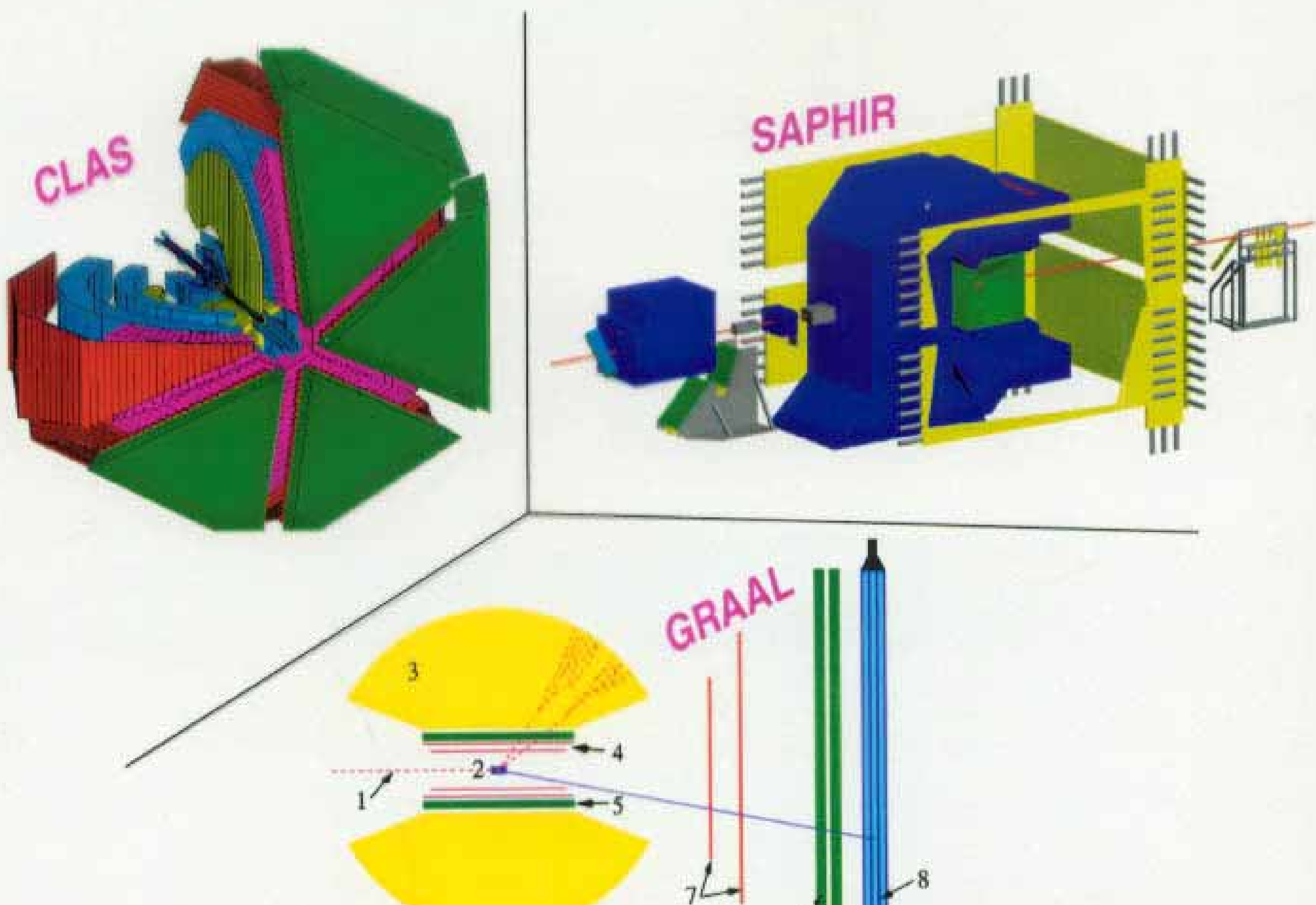

Outline

- Physics Motivation
- Facilities and Programs
- Formalism and Models
- Physics Results for Λ and Σ^0

  (Samples)

  Photo and Electroproduction

  Cross section and polarization data
- Summary and Outlook

The Baryon Resonances

- The constituent quark model provides a reasonable description of the known baryons.

More states predicted than seen experimentally.

Baryon	*** and **** Resonances	* and ** Resonances
N^*	$S_{11}(1535)$, $S_{11}(1650)$, $P_{11}(1440)$, $P_{11}(1710)$, $P_{13}(1720)$, $D_{13}(1520)$, $D_{13}(1700)$, $D_{15}(1675)$, $F_{15}(1680)$, $G_{17}(2190)$, $G_{19}(2250)$, $H_{19}(2220)$	$S_{11}(2090)$, $P_{11}(2100)$, $P_{13}(1900)$, $D_{13}(2080)$, $D_{15}(2200)$, $F_{15}(2000)$, $F_{17}(1990)$
Λ^*	$S_{01}(1405)$, $S_{01}(1650)$, $S_{01}(1800)$, $P_{01}(1600)$, $P_{01}(1810)$, $P_{03}(1890)$, $D_{03}(1520)$, $D_{03}(1690)$, $D_{05}(1830)$, $F_{05}(1820)$, $F_{05}(2110)$, $G_{07}(2100)$, $H_{09}(2350)$	$D_{03}(2325)$, $F_{07}(2020)$
Σ^*	$S_{11}(1750)$, $P_{11}(1660)$, $P_{11}(1880)$, $P_{13}(1385)$, $D_{13}(1670)$, $D_{13}(1940)$, $D_{15}(1775)$, $F_{15}(1915)$, $F_{17}(2030)$	$S_{11}(1620)$, $S_{11}(2000)$, $P_{11}(1710)$, $P_{11}(1880)$, $P_{13}(1840)$, $P_{13}(2080)$, $D_{13}(1580)$, $F_{15}(2070)$, $G_{17}(2100)$

B. Saghai, nucl-th/0105001

- Maybe N* states can decay through channels such as KY.
  - This seems to be supported by recent data. (SAPHIR, GRAAL, CLAS)
  - In accord with recent quark model calculations. Ref: Capstick and Roberts, PRD 58 (1998).

S_{11} (1650), P_{11} (1710), P_{13} (1720), D_{13} (1900)

Why Strangeness Production?

- Search for "missing" baryon resonances.
  - Not strongly produced by pion beams.
  - Focus on $W \gtrsim 2$ GeV. (Fertile area for discovery)
  - Λ / Σ^0 selection acts as isospin filter.
  - Competitive with multi–pion decay studies.

- Study structure of intermediate mesons and baryons.
  - Determine masses, widths, helicity amplitudes, and partial decay widths.

- Access to polarization observables.
  - Λ / Σ^0 decays are self–analyzing.
  - Polarized beams $\Longrightarrow$ double–polarization.

Multi–Laboratory Effort

SPring–8 : – Polarized photon facility in Hyogo
– Forward–angle hodoscope (small t physics)
– 8 GeV photons

SAPHIR : – Large acceptance detector in Bonn
– 1 – 3 GeV tagged–photon beam

GRAAL: – Polarized photon facility in Grenoble
– Large solid angle detector
– 0.5 – 1.5 GeV photons

Jefferson Laboratory (1 – 6 GeV CW polarized electrons)

Hall C : – Dual spectrometer system

Hall A : – Dual spectrometer system
– Extends Hall C physics to higher Q^2

Hall B : – CLAS large acceptance spectrometer
– For use with photon and electron beams

** Polarized targets are also part of several experiments. **

The Programs

Accelerator	Detector	Beam	Final State	Analysis
BONN/ELSA	SAPHIR	γ	$K^+(\Lambda,\Sigma)$	Cross sections
			$K^+(\Lambda,\Sigma)p$	Induced polarization
ELFE	GRAAL	$\vec{\gamma}$	$K^+(\Lambda,\Sigma)$	Cross sections
			$K^+(\Lambda,\Sigma)p$	Single/Double polarization
JLab/CEBAF	Halls A+C	e	$eK^+(\Lambda,\Sigma)$	σ_L/σ_T
	CLAS	e	$eK^+(\Lambda,\Sigma)$	σ_L/σ_T, σ_{LT}, σ_{TT}
		γ	$K^+(\Lambda,\Sigma)p$	Induced polarization
		$\vec{\gamma}$	$K^+(\Lambda,\Sigma)p$	Single/Double polarization
		e	$eK^+(\Lambda,\Sigma)p$	Induced polarization
		$\vec{e}$	$eK^+(\Lambda,\Sigma)p$	Single/Double polarization
		γ	$K^{*+}(\Lambda,\Sigma)$	Cross sections
		e	$eK^{*+}(\Lambda,\Sigma)$	Cross sections

Not a complete list ...

Tight constraints

"Missing" N* Resonances

- In the absence of direct QCD predictions:

Use effective theories to model reaction mechanism.

$\gamma + p \rightarrow K^+ + \Lambda$

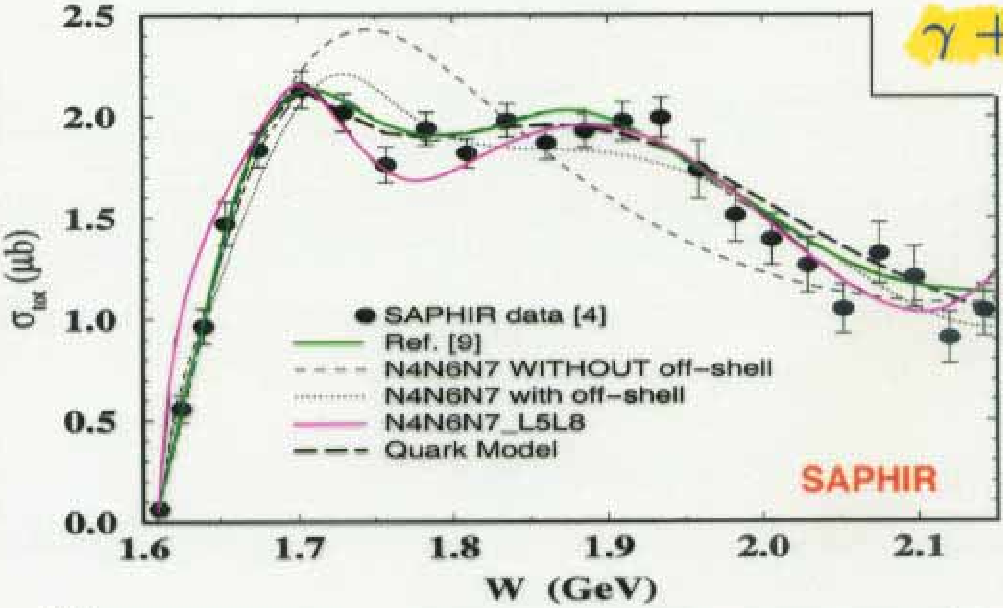

Ref. B. Saghai
nucl-th/0105001

D_{13} (1895) Study

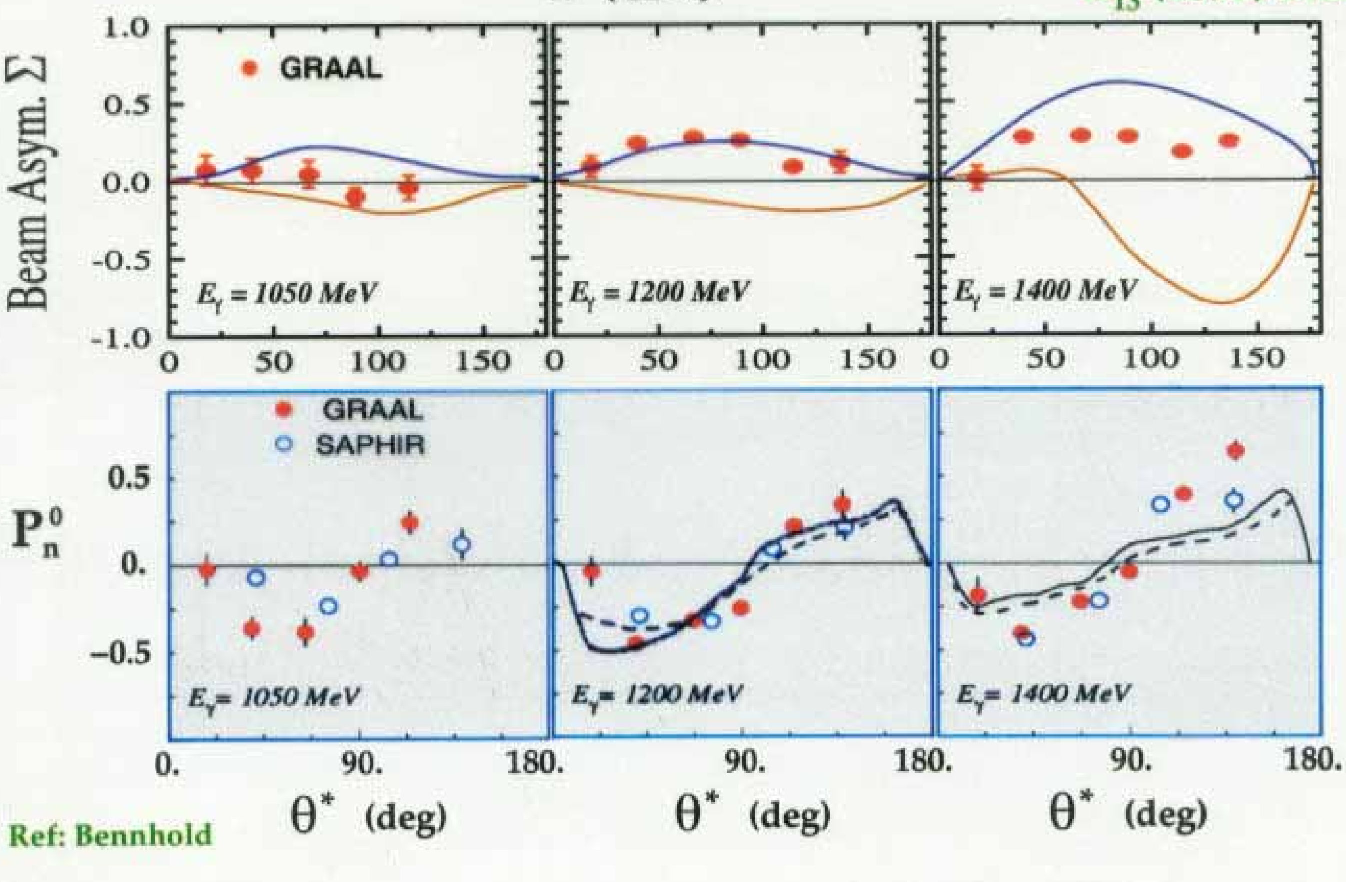

Ref: Bennhold

Reaction Dynamics

- **What are the production dynamics?**

Measure:

- Cross sections
- Polarization observables

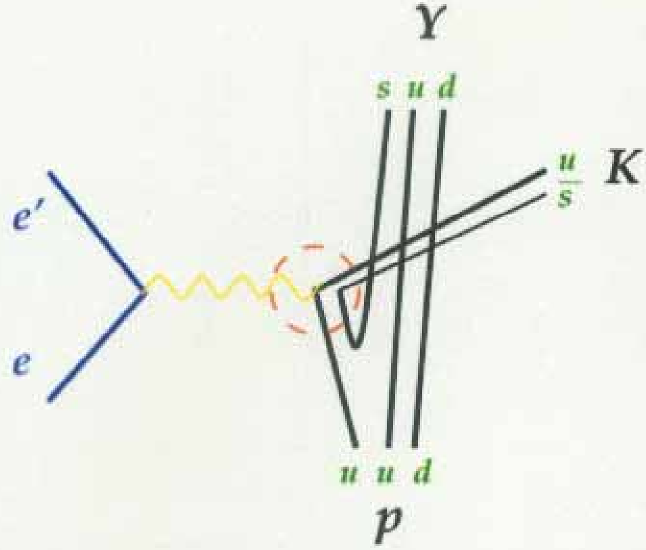

meson exchange

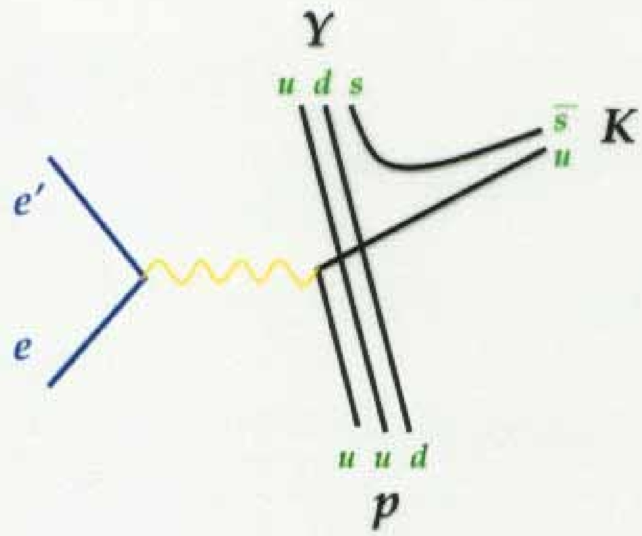

N creation/decay*

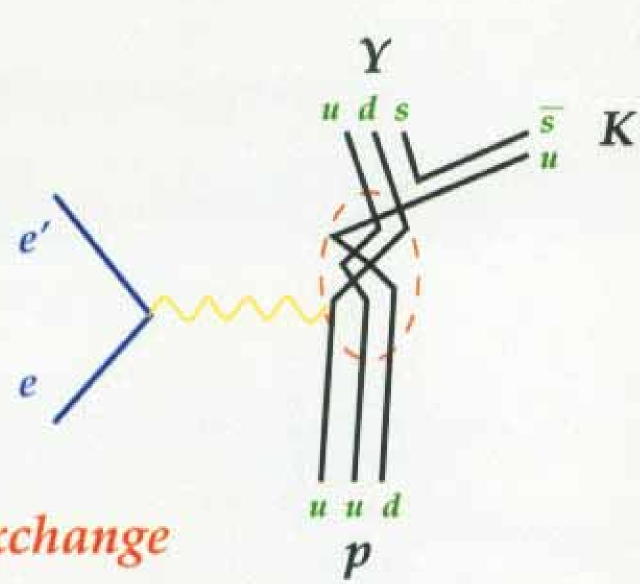

hyperon exchange

Model Introduction

- Hadrodynamic Models:
  - Models based on including a number of s–, t–, and u–channel diagrams.

    Born terms and various resonances.
  - t–channel contains only K and K*.
  - Coupling strengths set by fits to existing data.
  - Features primarily due to s–channel resonances.
  - Effective at low to moderate energies.

- Regge Models:
  - Parameterized t–channel exchange (Regge).
  - No s–channel resonances included (only Born terms).
  - Very few adjustable parameters.
  - Effective at moderate (2 GeV and above) energies.

Formalism

$$\frac{d^5\sigma}{d\Omega_{E'} d\Omega_K^* dE'} = \Gamma_v \frac{d^2\sigma_v}{d\Omega_K^*}$$

$$\frac{d^2\sigma_v}{d\Omega_K^*} = \sigma_0 \left[1 + h\ A_{TL'} + \vec{S} \cdot \vec{P}^0\ +\ h\ (\vec{S} \cdot \vec{P}')\right]$$

Unpolarized Cross Section

$$\sigma_0 = \sigma_T + \epsilon_L \sigma_L + \epsilon \sigma_{TT} \cos 2\Phi + \sqrt{2\epsilon_L(1+\epsilon)}\ \sigma_{TL} \cos \Phi$$

$$A_{TL'} = \frac{K_{CM}}{\sigma_0} \sqrt{2\epsilon_L(1-\epsilon)}\ R_{TL'}^{00} \sin \Phi$$

Polarized beam

Hyperon polarization

Induced

$$\begin{pmatrix} P_t^0 \\ P_n^0 \\ P_\ell^0 \end{pmatrix} = \frac{K_{CM}}{\sigma_0} \begin{pmatrix} -\sqrt{2\epsilon_L(1+\epsilon)}\ R_{TL}^{x'0} \sin \Phi - \epsilon R_{TT}^{x'0} \sin 2\Phi \\ R_T^{y'0} + \epsilon_L R_L^{y'0} + \sqrt{2\epsilon_L(1+\epsilon)}\ R_{TL}^{y'0} \cos \Phi + \epsilon R_{TT}^{y'0} \cos 2\Phi \\ -\sqrt{2\epsilon_L(1+\epsilon)}\ R_{TL}^{z'0} \sin \Phi - \epsilon R_{TT}^{z'0} \sin 2\Phi \end{pmatrix}$$

Transferred

$$\begin{pmatrix} P_t' \\ P_n' \\ P_\ell' \end{pmatrix} = \frac{K_{CM}}{\sigma_0} \begin{pmatrix} -\sqrt{2\epsilon_L(1-\epsilon)}\ R_{TL'}^{x'0} \cos \Phi - \sqrt{1-\epsilon^2}\ R_{TT'}^{x'0} \\ \sqrt{2\epsilon_L(1-\epsilon)}\ R_{TL'}^{y'0} \sin \Phi \\ -\sqrt{2\epsilon_L(1-\epsilon)}\ R_{TL'}^{z'0} \cos \Phi - \sqrt{1-\epsilon^2}\ R_{TT'}^{z'0} \end{pmatrix}$$

Photoproduction Data

- *Total cross sections*
- *Differential cross sections*
- *Induced polarization*
- *Measure both Λ,Σ*

Total Cross Sections

$\gamma + p \rightarrow K^+ + \Lambda$

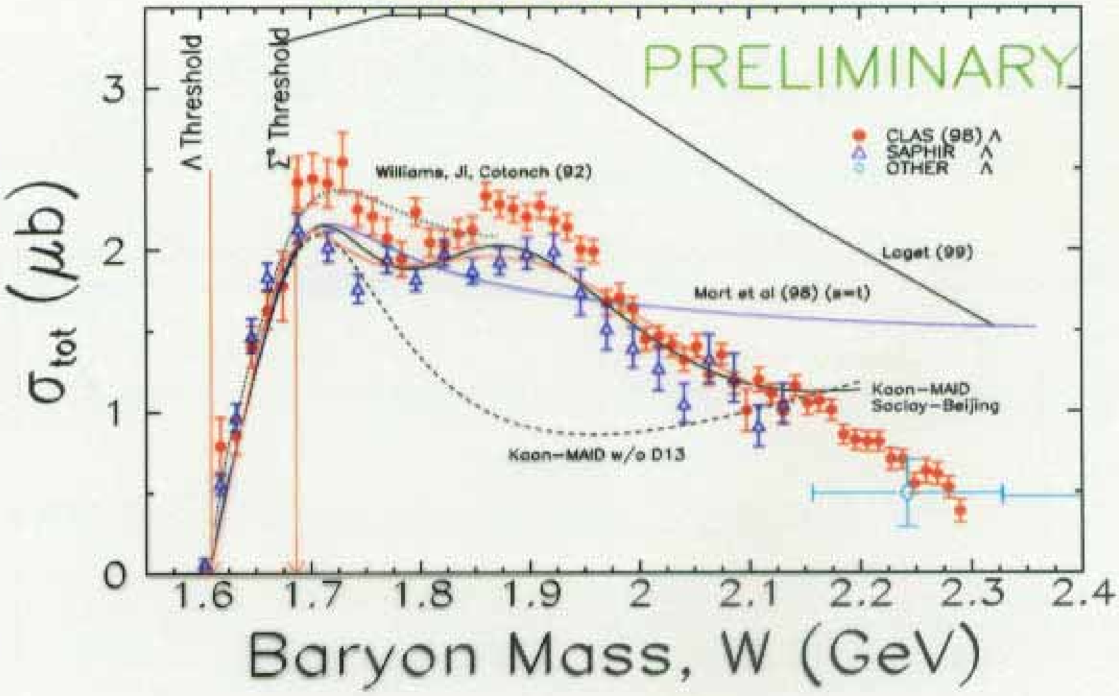

$\gamma + p \rightarrow K^+ + \Sigma^0$

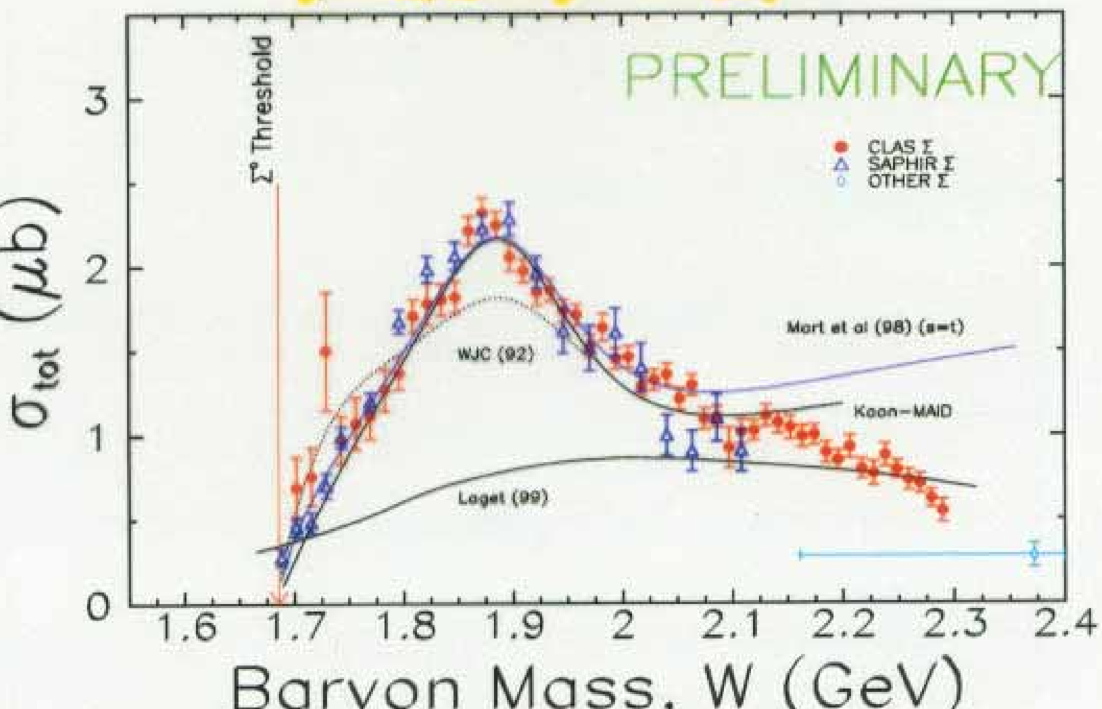

R.A. Schumacher

Energy Distributions

$\gamma + p \rightarrow K^+ + \Lambda$

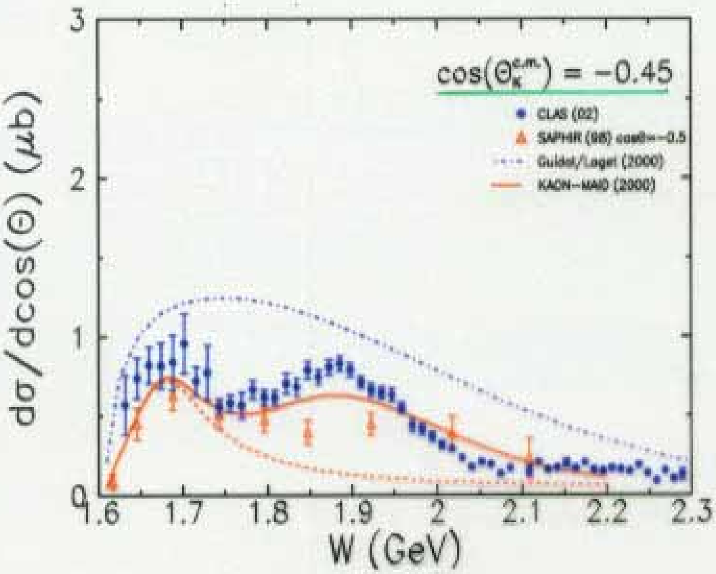

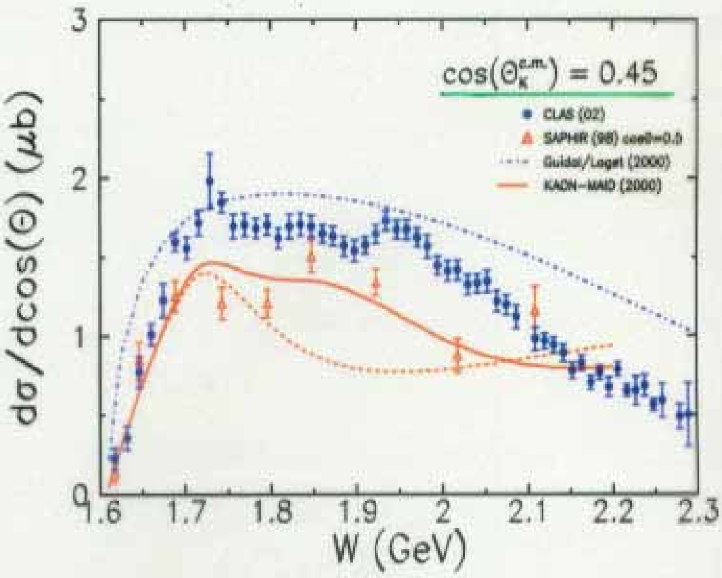

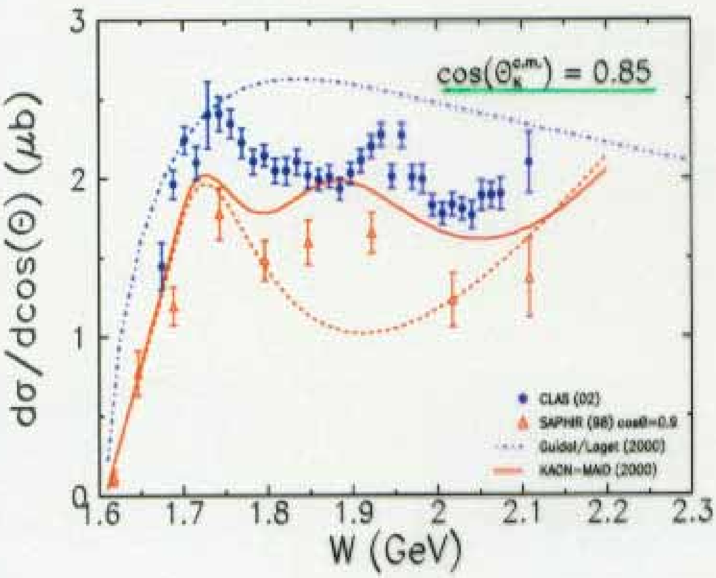

Hadrodynamic model (GWU)
Regge model (Laget, Guidal)

– **Sample of 921 CLAS points.**

– **M=1890 MeV, Γ=200 MeV back–angle peak seen**

– **M=1950 MeV, Γ=100 MeV forward angle peak seen**

– **Existing models perform poorly**

R.A. Schumacher

Energy Distributions

$\gamma + p \rightarrow K^+ + \Sigma^0$

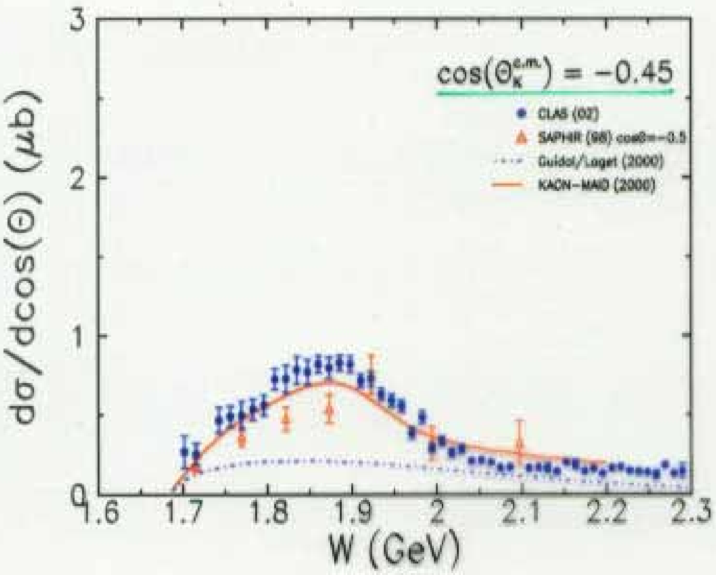

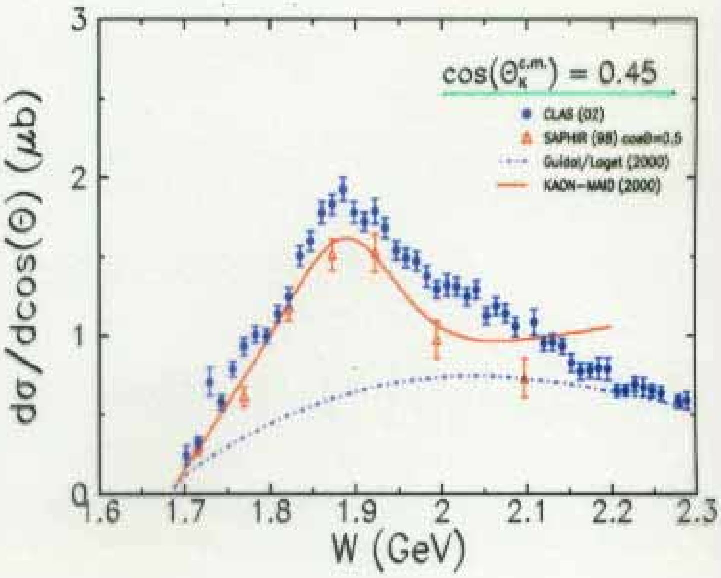

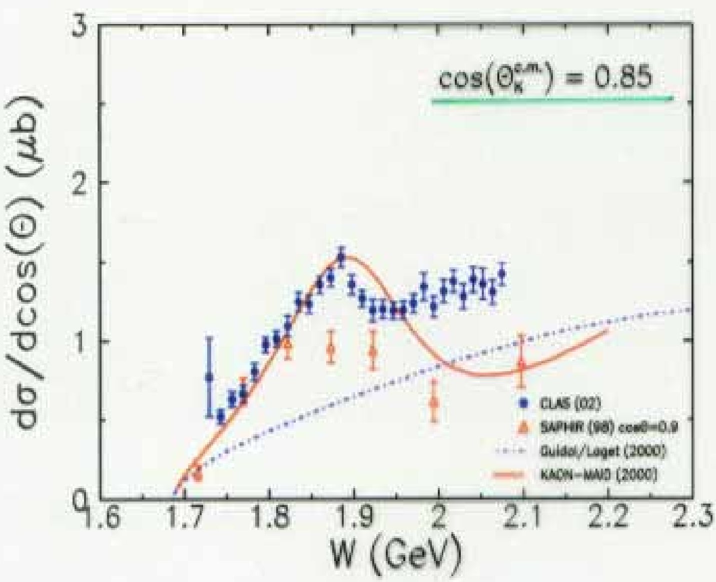

Hadrodynamic model

Regge model

– Sample of 782 CLAS points.

– One peak near 1900 MeV with angle–dependent shape

– Existing models perform poorly

R.A. Schumacher

Induced Polarization

$\gamma + p \rightarrow K^{+} + \Lambda$

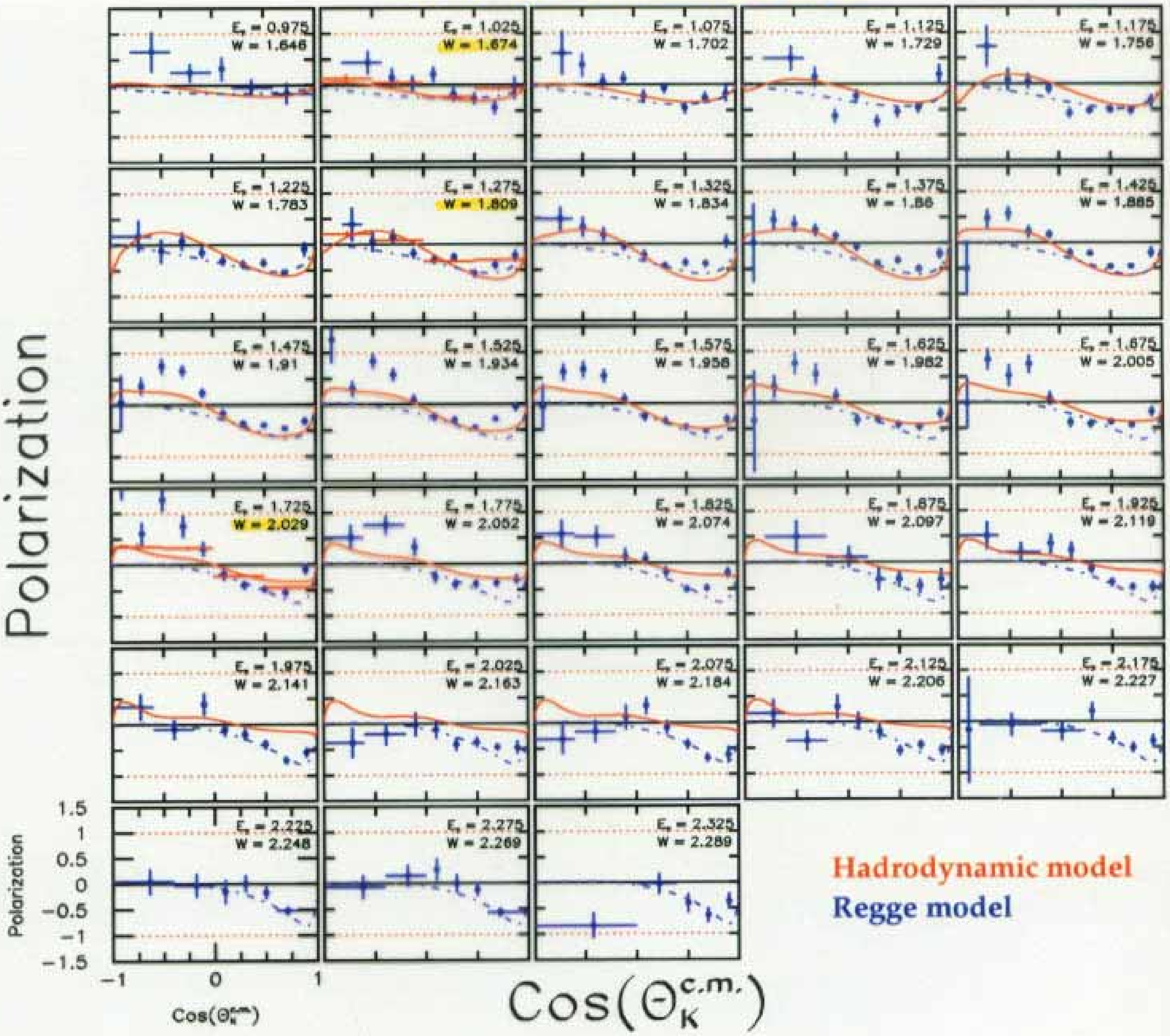

- Full CLAS data set (blue)
- Fair agreement with SAPHIR data (red)
- Deviations apparent with models over full kinematics

R.A. Schumacher

Induced Polarization

$$\gamma + p \rightarrow K^+ + \Sigma^0$$

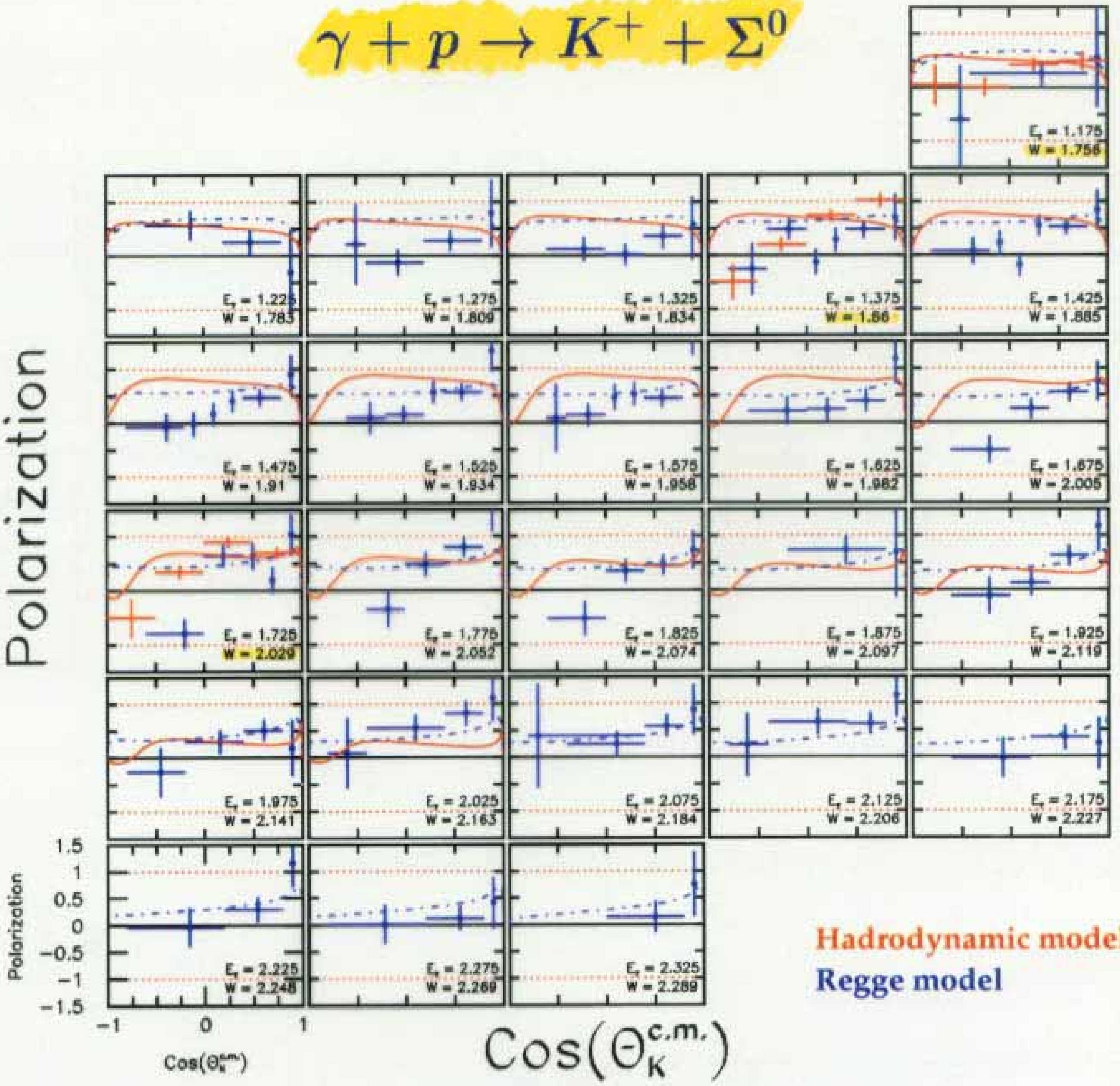

Hadrodynamic model

Regge model

- Full CLAS data set (blue)
- Fair agreement with SAPHIR data (red)
- Deviations apparent with models over full kinematics

R.A. Schumacher

Electroproduction Data

- *Unpolarized structure functions*
- *Beam asymmetries*
- *Induced polarization*
- *Transferred polarization*
- *Measure both* Λ,Σ

Structure Functions

$$\sigma_0 = \sigma_T + \epsilon_L \sigma_L + \epsilon \sigma_{TT} \cos 2\Phi + \sqrt{2\epsilon_L(1+\epsilon)}\, \sigma_{TL} \cos \Phi$$

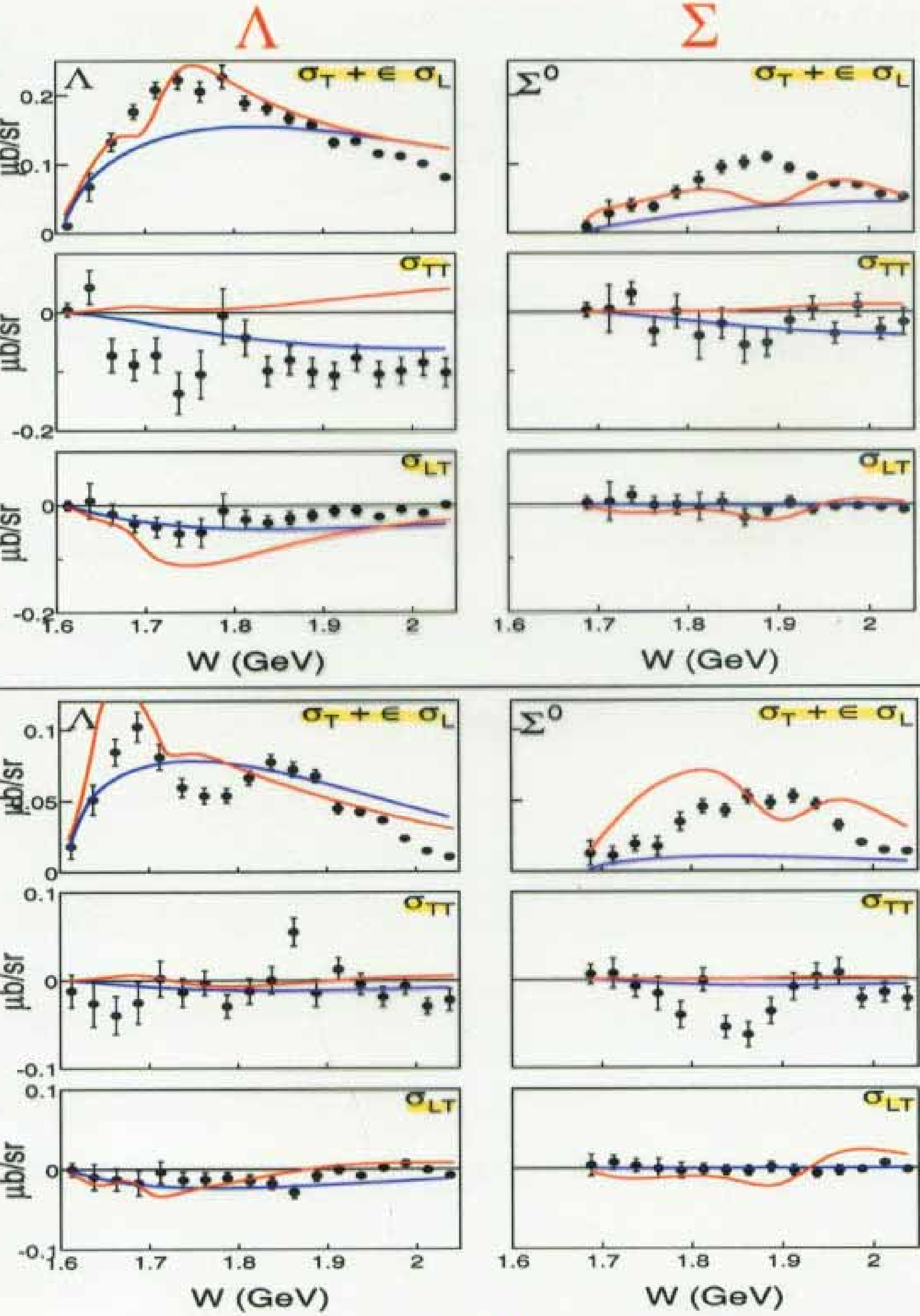

CLAS

Forward angle bin

$\cos\theta^*_K$: (0.3,0.7)

Backward angle bin

$\cos\theta^*_K$: (−0.7:−0.3)

Regge

Hadrodynamic

(2.6 GeV, Q^2: 0.5–0.9 GeV^2)

Structure Functions

$$\sigma_0 = \sigma_T + \epsilon_L \sigma_L + \epsilon \sigma_{TT} \cos 2\Phi + \sqrt{2\epsilon_L(1+\epsilon)}\, \sigma_{TL} \cos \Phi$$

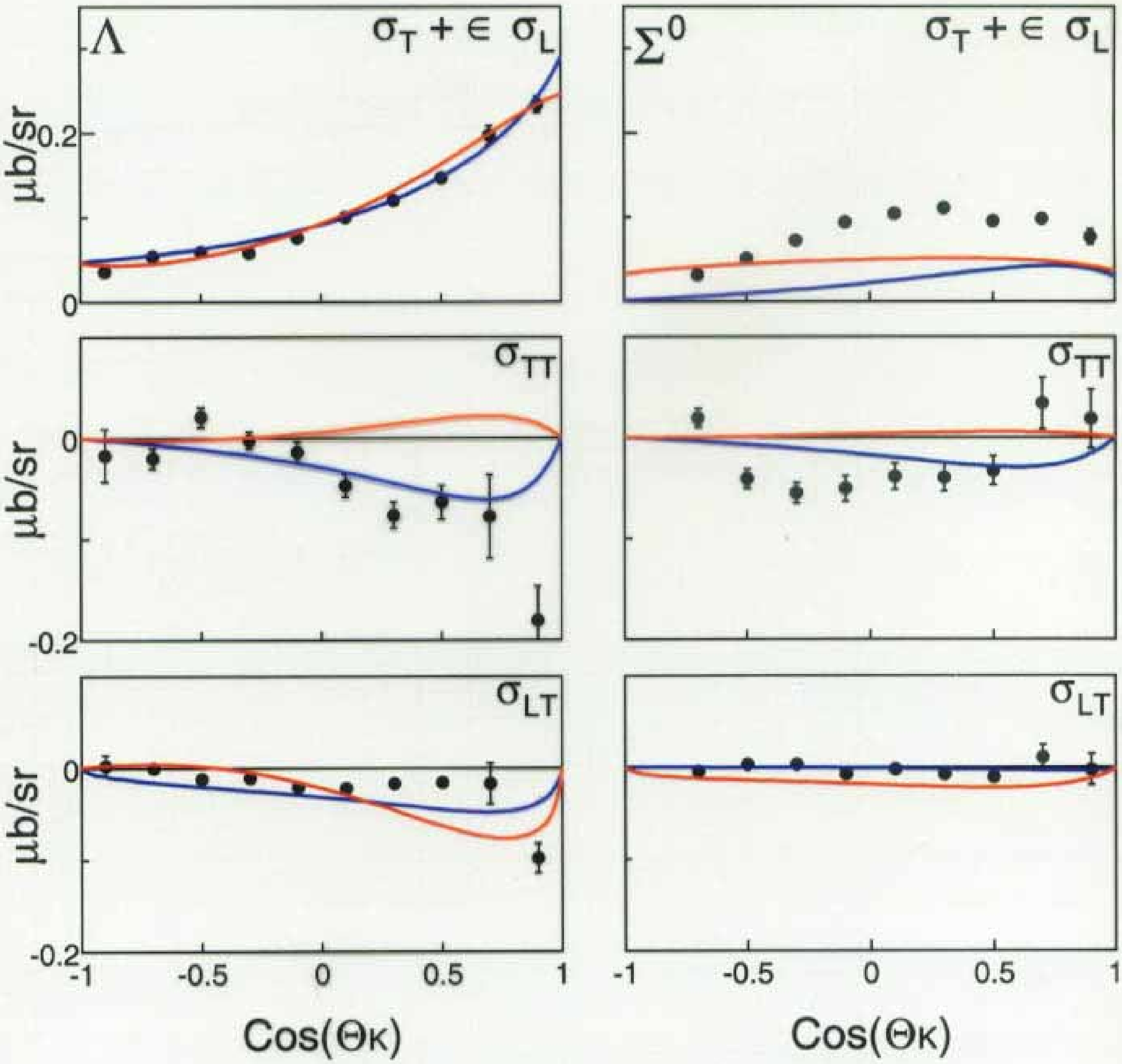

W=1.85–1.95 GeV

Regge
Hadrodynamic

(2.6 GeV, Q^2: 0.5–0.9 GeV^2)

Beam Asymmetry

- **Measure polarized beam asymmetry.** **(fifth structure function)**

$$A_{TL'} = \frac{1}{P_e}\frac{N^+ - N^-}{N^+ + N^-} = \frac{1}{\sigma_0}\sqrt{2\epsilon_L(1-\epsilon)}\,\sigma_{TL'}\sin\Phi$$

Allows study of resonant–nonresonant interference.

$$\vec{e} + p \rightarrow e' + K^+ + \Lambda$$

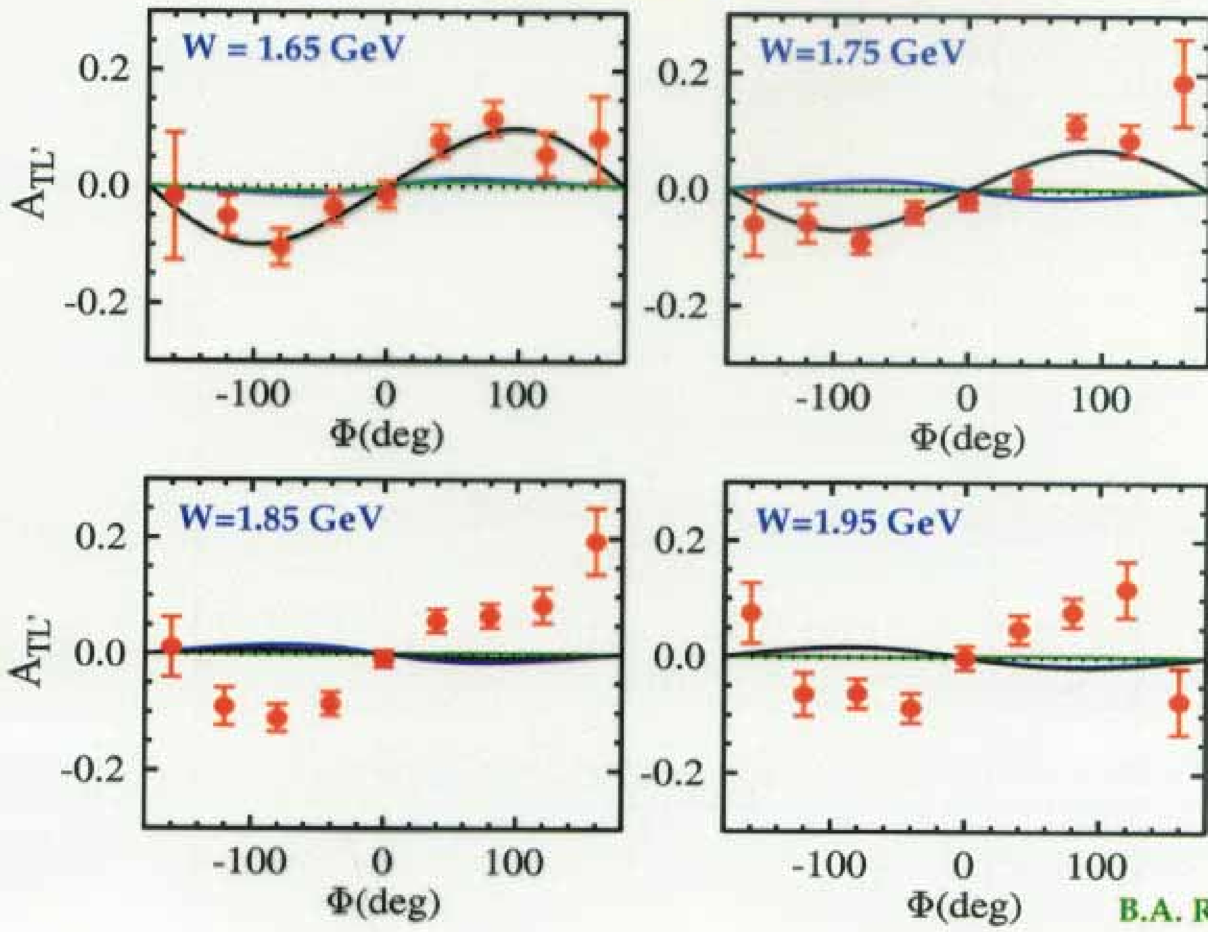

B.A. Raue

Williams, Ji, Cotanch – 1992
Bennhold and Mart – 1998
Bennhold and Mart – 2002

2.567 GeV
Summed over Q^2

Induced Polarization

$e + p \rightarrow e' + K^+ + \Lambda$

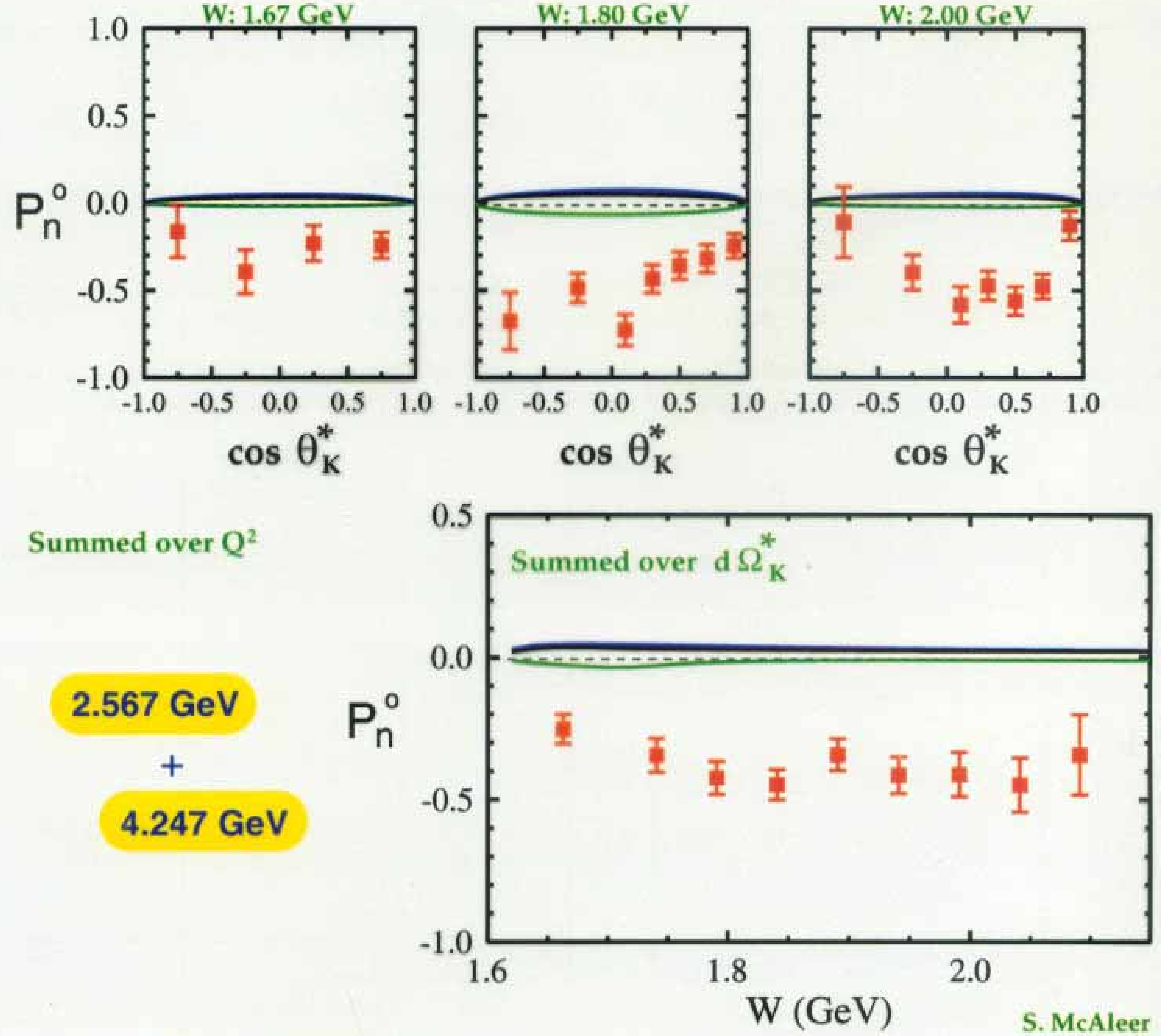

2.567 GeV
+
4.247 GeV

Adelseck and Wright – 1988
Bennhold and Mart – 1998
Cotanch – 1992

Comparison to photoproduction:

Similar energy dependence
Much different angular dependence

Transferred Polarization

$\vec{e} + p \rightarrow e' + K^+ + \vec{\Lambda}$

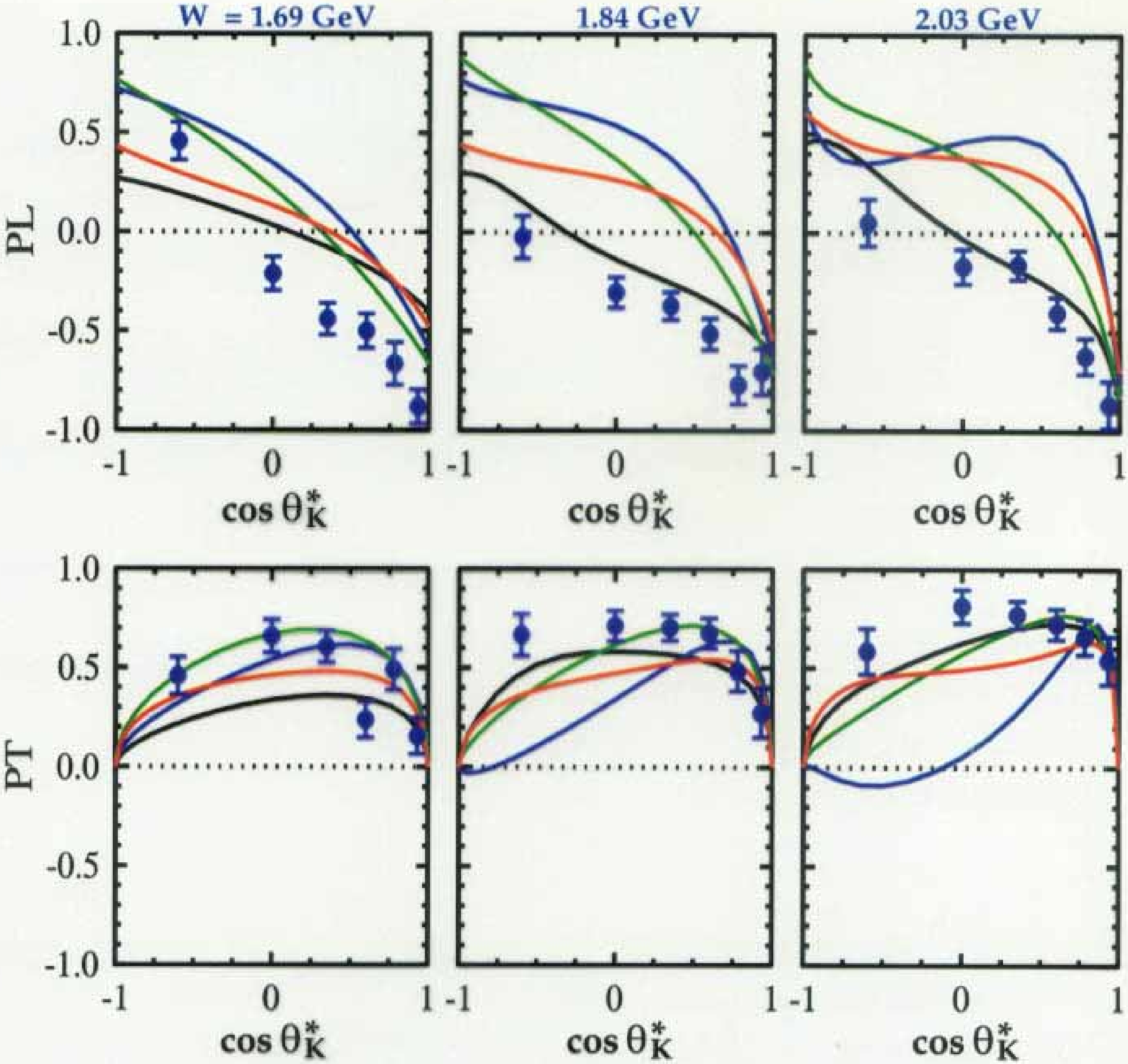

Adelseck and Wright – 1988
Cotanch – 1992
Mart and Bennhold – 2002
Janssen – 2002

2.567 GeV
Summed over Q^2, Φ

Transferred Polarization

$$\vec{e} + p \rightarrow e' + K^+ + \vec{\Lambda}$$

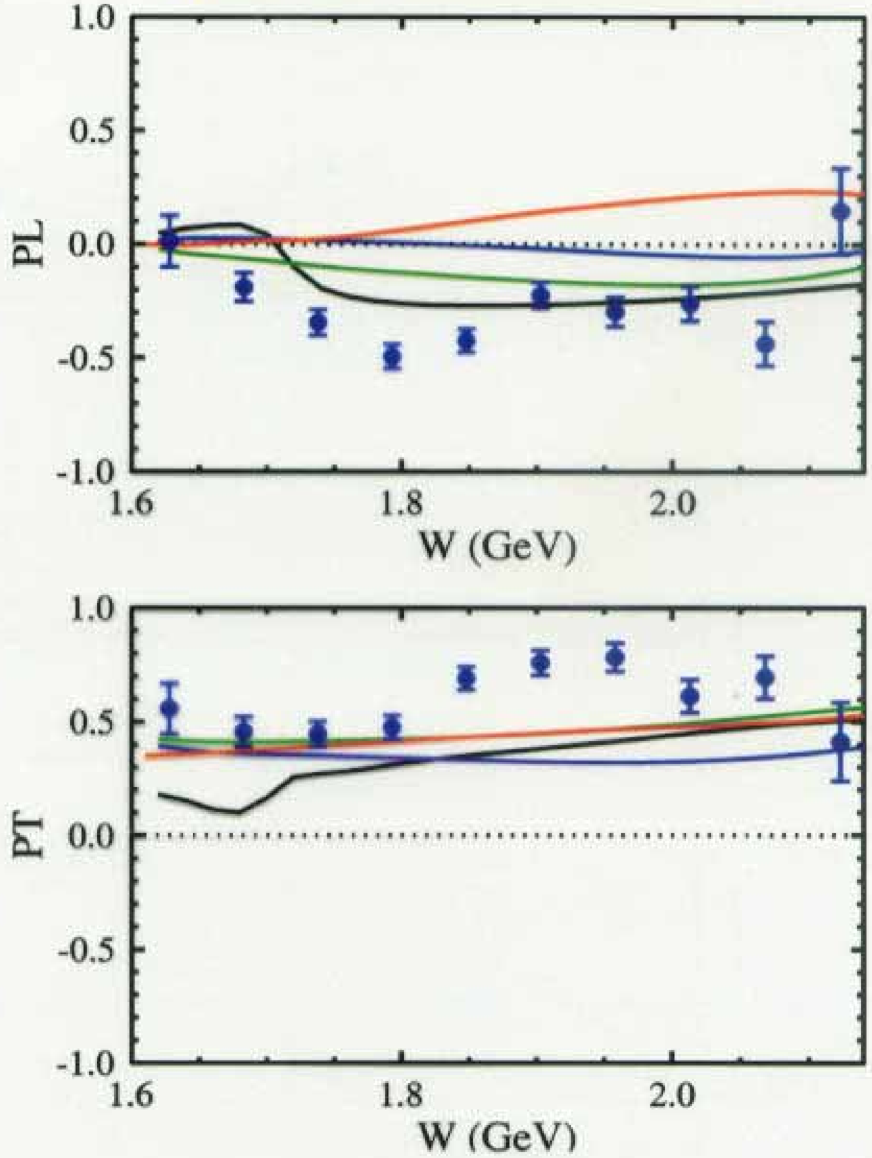

Adelseck and Wright – 1988
Cotanch – 1992
Bennhold and Mart – 2002
Janssen – 2002

2.567 GeV
Summed over Q^2, $d\Omega_K^*$

Summary/ Conclusions

- Associated Strangeness Production Data:

  – Sensitive to high–mass baryons (>1.6 GeV) with large K–Y couplings.

  – New high quality data becoming available from a number of different facilities.

  Cross sections and spin observables.

  Key goals to understand nucleon structure and the spectrum of excited states.

  – Clear evidence of resonant structures in the energy and angle dependences.

  – Existing theoretical models do not describe the data well over the broad kinematic phase space measured.

  └ Productive new round of fitting/modeling

  Improved PWA analysis now possible.

Wealth of data $\Longrightarrow$ Tight constraints